MOLECULAR AND CELLULAR BIOLOGY, Dec. 2007, p. 8340–8351 Vol. 27, No. 23
0270-7306/07/$08.00+0 doi:10.1128/MCB.00972-07

ZBP2 Facilitates Binding of ZBP1 to β-Actin mRNA during Transcription▽†

Feng Pan,‡ Stefan Hüttelmaier,§ Robert H. Singer,* and Wei Gu

Department of Anatomy and Structural Biology and Department of Cell Biology, Albert Einstein College of Medicine, 1300 Morris Park Ave., Bronx, New York 10461

Received 1 June 2007/Returned for modification 2 July 2007/Accepted 12 September 2007

Cytoplasmic mRNA localization regulates gene expression by spatially restricting protein translation. Recent evidence has shown that nuclear proteins (such as hnRNPs) are required to form mRNPs capable of cytoplasmic localization. ZBP1 and ZBP2, two hnRNP K homology domain-containing proteins, were previously identified by their binding to the zipcode, the sequence element necessary and sufficient for β-actin mRNA localization. ZBP1 colocalizes with nascent β-actin mRNA in the nucleus but is predominantly a cytoplasmic protein. ZBP2, in contrast, is predominantly nuclear. We hypothesized that the two proteins cooperate to localize β-actin mRNA and sought to address where and how this might occur. We demonstrate that ZBP2, a homologue of the splicing factor KSRP, binds initially to nascent β-actin transcripts and facilitates the subsequent binding of the shuttling ZBP1. ZBP1 then associates with the RNA throughout the nuclear export and cytoplasmic localization process.

Cells are organized into discrete compartments harboring distinct complements of proteins. There are several mechanisms to sort proteins to their proper destinations. One way is to localize mRNA to the compartment where its protein products are needed (31). This mechanism is widely used to generate cell polarity and to target cell fate determinants in various organisms. *ASH1* mRNA is localized to the bud tip of dividing yeast so that the Ash1 protein is present only in daughter cell nuclei to promote mating type switching (39, 50). During *Drosophila* oogenesis and embryogenesis, morphogen mRNAs are targeted to specific parts of oocytes or embryos to dictate the future direction of differentiation (29, 30). In developing neurons, cytoskeleton component mRNAs, such as β-actin, MAP2, and arc mRNAs, are transported into dendrites and/or growth cones, where their protein products are involved in rapid cytoskeleton dynamics important for neurite growth and plasticity (4, 40, 53). Proper localization of β-actin mRNA to the leading edge of chicken embryo fibroblasts (CEFs) and growth cones of developing neurons is important for maintenance of cell polarity and directed cell motion (18, 48). mRNAs localize through a *cis*-acting signal(s), termed a zipcode(s), which resides mostly in their 3′ untranslated regions (UTRs). β-Actin localization is dependent on a 54-nucleotide (nt) zipcode located in the 3′ UTR (32, 33, 40, 53). Several categories of *trans*-acting factors required for mRNA localization have been identified, including zipcode binding proteins, motor proteins, and scaffolding proteins (3, 44). A predominantly cytoplasmic protein, zipcode binding protein 1 (ZBP1), was identified by its association with the β-actin zipcode (23, 47). A second zipcode binding protein, ZBP2, was identified from chicken embryo brain extract by RNA affinity chromatography (23). The protein is a chicken homologue of human KH domain-containing splicing regulatory protein (KSRP) (41). KSRP is also known as fuse binding protein 2 (FBP), one of three vertebrate FBP family members (13, 41) found to participate in many steps of RNA metabolism, including transcription (14), pre-mRNA splicing (1, 25, 36, 41), mRNA editing (38), and exosome-mediated mRNA degradation (6, 20). Protein sequences of many known FBP family members were aligned to generate a phylogenetic tree (see Fig. S1 in the supplemental material). Several ZBP2 orthologues from different species are implicated in RNA localization. Overexpression of RNA binding KH domains of ZBP2 partially delocalized β-actin mRNA in both CEFs and developing neurons (23). A rat homologue of ZBP2, MARTA1, was identified by its association with the dendritic targeting element of MAP2 mRNA (45). Rat ZBP2 also bound to the β-actin zipcode and an AU-rich element that mediates rapid RNA decay (49). Recently, mouse ZBP2 (mKSRP) functioning as a major molecular determinant of β-catenin mRNA instability has been reported (21). VgRBP71, the *Xenopus* orthologue of ZBP2, was identified by virtue of its binding to *Vg1* mRNA localizing element (35). These observations suggest that ZBP2 is utilized in evolutionally conserved pathways to target different mRNA targets in both germ line and somatic cells.

Although substantial data demonstrated that ZBP1 and ZBP2 are involved in β-actin mRNA localization, several questions remain to be addressed. First, most ZBP1 and ZBP2 are in separate compartments although a small fraction of ZBP1 can be detected at β-actin transcription sites (28, 42) and some ZBP2 can be found in the cytoplasm (23, 45). We hypothesized that these two proteins engage in transient interactions to direct the fate of the β-actin mRNA from the nucleus into the

* Corresponding author. Mailing address: Department of Anatomy and Structural Biology and Department of Cell Biology, Albert Einstein College of Medicine, 1300 Morris Park Ave., Bronx, NY 10461. Phone: (718) 430-8646. Fax: (718) 430-8697. E-mail: rhsinger@aecom.yu.edu.

† Supplemental material for this article may be found at http://mcb.asm.org/.

‡ Present address: Molecular Neurobiology Program, Skirball Institute, New York University Medical Center, New York, NY 10016.

§ Present address: Martin-Luther Universität Halle, ZAMED, Heinrich Damerow Str. 1, 06120 Halle (Saale), Germany.

▽ Published ahead of print on 24 September 2007.

cytoplasm. Second, ZBP2 and ZBP1 both bind to the wild-type zipcode but not a mutated zipcode (23, 47). Hence, they may either compete for or cooperatively bind to a single RNA molecule. Third, the binding of one protein to the zipcode could be a prerequisite for the other protein to bind efficiently.

In this work, we provide evidence for the hypothesis that the two zipcode binding proteins, ZBP2 and ZBP1, act cooperatively. The evidence demonstrates that ZBP2 is recruited to β-actin mRNA transcription sites in the nucleus, and this event is required for the efficient binding of ZBP1 to nascent mRNA. We propose that this cooperation on nascent chains of β-actin mRNA regulates the formation of localizable mRNPs.

MATERIALS AND METHODS

Constructs. Three cDNA fragments of chicken ZBP2, KH1-2 (amino acids 195 to 373), KH3-4 (amino acids 374 to 557), and KH1-4 (amino acids 195 to 557), as well as the full-length protein were amplified by PCR and cloned into pTOPO cloning vectors (Invitrogen) for sequencing confirmation. These fragments were then cloned into appropriate pFASTBAC His-Tag vectors (Invitrogen) to express recombinant proteins. mZBP2 (see below) and human KSRP were also cloned into fluorescent protein vectors (Clontech) for transient transfections.

Northern blotting and quantification analysis. A 451-nt cDNA fragment encoding the carboxyl terminus of human KSRP was ^{32}P labeled using Stratagene's random labeling kit and was used as probe to detect KSRP expression. This fragment was chosen because it shared low homology with other ZBP2 family members. The human β-actin full-length open reading frame was labeled as a probe for actin mRNA detection. The human multitissue blot (Clontech) was hybridized in Stratagene's QuickHyb buffer according to the manufacturer's instructions. The blot was exposed to X-ray film or a phosphorimager and quantified with Storm (Amersham Biosciences) software.

Protein purification. His-tagged chicken ZBP2 and various KH domain fragments were cloned into pFASTBAC vectors and expressed in SF9 insect cells according to Invitrogen's manual. Briefly, ZBP2 constructs and packaging helper phage were transfected into adherent SF9 cells of variable confluence. Accumulated phage particles were collected after 72 h. High-titer supernatant was then used to infect fast-growing SF9 cells. Cells were collected 48 h after infection. Cell lysates were obtained by brief sonication and ultracentrifugation. His-tagged proteins were then purified using Ni-nitrilotriacetic acid beads (QIAGEN). Full-length ZBP1 and KH1-4 fragment were cloned into pGEX6P-1 at EcoRI and XhoI sites (Amersham Bioscience) and purified. Crude His-tagged proteins and glutathione *S*-transferase fusion proteins were further purified by fast protein liquid chromatography using HiTrap heparin HP columns (Amersham Biosciences).

In vitro RNA binding assays. (i) Gel mobility shift assay. ^{32}P-labeled chicken zipcode of β-actin mRNA was generated from linearized plasmids using the SP6 RNA in vitro transcription kit (Promega). Gel shift reactions were performed as previously described (23).

(ii) Nitrocellulose filter binding assays. Filter binding assays (5) were used to measure the binding dissociation constants between the zipcode RNA and recombinant ZBP2 or its truncations. Binding reaction mixtures (50 μl) contained the following: 200 mM K acetate, 50 mM Tris acetate (pH 7.7), 5 mM Mg acetate, 10,000 cpm labeled zipcode RNA, and threefold serially diluted recombinant ZBP2 protein fragments. Reaction mixtures were incubated for 10 min at room temperature, followed by filtering (Millipore HAWP 25-mm filter/1225 Sampling Manifold) and washing. The fraction of bound RNA was plotted graphically versus the log of protein concentration to determine dissociation constants (19).

(iii) SELEX. Systematic evolution of ligands by exponential enrichment (SELEX) experiments for ZBP2 were performed as described previously (19).

RNase footprinting assay. The 54-nt chicken β-actin zipcode was in vitro transcribed and purified by 6% denaturing urea-polyacrylamide gel electrophoresis (PAGE) and eluted in buffer containing 1 M ammonium acetate and 1% sodium dodecyl sulfate (SDS) overnight at 37°C. Purified RNA was 5′ dephosphorylated and ^{32}P labeled using Ambion's end labeling kit according to the manufacturer's protocols. Labeled RNA probe (10,000 cpm) was incubated with different concentrations of ZBPs for 30 min, followed by 10 min of RNase V1 (Ambion) digestion (0.1 unit/20 μl). The mixtures were resolved by 12% urea-PAGE with an alkaline-hydrolyzed probe as a size ladder.

Cloning of the mZBP2 gene. The mouse expressed sequence tag database was queried with human KSRP, FBP1, and FBP3 sequences. Several clones showed high homology to KSRP but not to FBP1 or FBP3. One clone (IMAGE no. 6335620) was ordered and sequenced. It contains a full open reading frame of 2,247 bp and about 1.3 kb of 3′ UTR. Since several expressed sequence tag clones omit about 100 bp of coding sequence near the start codon, PCR amplification of the N-terminal region was done using Clontech's mouse embryo marathon ready cDNA (catalog no. 7458-1) as the template. The PCR product was cloned into the pTOPO vector. Several clones were sequenced, and all of them contained the 100-bp region.

Cell culture and transfection. CEFs were cultured in minimal essential medium with 10% fetal bovine serum (FBS) as previously described (23). NG108-15 cells were maintained in Dulbecco's modified Eagle medium (DMEM) with 1× hypoxanthine-aminopterin-thymidine (Sigma) and 10% FBS. Differentiated NG108-15 cells were initiated in DMEM with 0.1× hypoxanthine-aminopterin-thymidine and 1% FBS for 12 to 24 h. 293 cells were cultured in DMEM with 10% FBS. Various cDNA constructs expressing ZBP2 or ZBP1 were transfected into these cultured cells with Lipofectamine 2000 (Invitrogen) or Nucleofector (Amaxa).

Immunofluorescence and in situ hybridization. Immunofluorescence and in situ hybridization were performed as previously described (23). Monoclonal anti-KSRP antibody or rat polyclonal antibody against ZBP2 was diluted 1:1,000 in phosphate-buffered saline (PBS)–1% bovine serum albumin for immunofluorescence (25). When both immunofluorescence and in situ hybridization were performed on the same sample, a 10-min fixation using 5% paraformaldehyde after immunofluorescence was applied to avoid significant loss of antibody signal (43).

Microscopy and imaging. Cells were viewed under an Olympus BX61 fluorescence microscope equipped with an Olympus PlanApo60X, 1.4NA oil objective. Images were acquired with a Roper coolSNAP HQ cooled charge-coupled device camera (Roper Scientific) operated by the IPlab software package (Scanalytics, Inc). Quantification of arbitrary fluorescence units in RNA interference (RNAi) experiments was performed with IPlab.

RNAi. Double-stranded small interfering RNA (siRNA) oligonucleotides were designed with the software packages from Ambion Inc. and QIAGEN Inc. and synthesized by Dharmacon Inc. The sequences of the three oligonucleotides we designed were as follows: Z2-322, ATAACAACACTCCTGATTT; Z2-646, AG ATGATGCTGGATGACAT; and Z2-1981, AGTACTACAAGAAGCAAGC. siRNA was transfected into 293 cells or NG108-15 cells with Lipofectamine 2000 (Invitrogen). Cells were analyzed 24 to 72 h after transfection by either Western blotting, reverse transcription-PCR (RT-PCR), or imaging. Quantification of RNAi experiments was performed with IPlab software. The freehand tool was used to measure the fluorescence intensity in the nucleus as well as the cytoplasm. The ZBP2 nuclear signal was at least two times higher than the cytoplasmic signal. We considered that ZBP2 was knocked down if the nuclear signal was equal to or less than the cytoplasmic intensity.

Real-time RT-PCR analyses. RNA was isolated using the RNeasy minikit (QIAGEN) and RNase-free DNase set (QIAGEN) according to the manufacturer's protocol. cDNA was generated by reverse transcription via the Superscript first-strand synthesis kit (Invitrogen) using equal amounts of total RNA as the template. Real-time PCR was performed using TaqMan universal PCR master mix and gene-specific TaqMan Assay-on-Demand primers and probes on a Prism 7900HT sequence detection system and analyzed with SDS software (ABI).

Immunoprecipitation and Western blotting. Cell lysate was prepared either in radioimmunoprecipitation assay buffer (150 mM NaCl, 10 mM Tris [pH 7.2], 0.1% SDS, 1.0% Triton X-100, 1% deoxycholate, 5 mM EDTA) or in low-salt NP-40 buffer (150 mM NaCl, 50 mM Tris [pH 7.4], 0.5% NP-40) with freshly added complete protease inhibitor cocktail (Roche). Immunoprecipitation and Western blotting were performed as previously described (23).

ChIP. MTC cells were grown to 85% confluence in DMEM supplemented with 10% FBS for 3 days either after being transfected for 12 h with ZBP2 siRNAs (chromatin immunoprecipitation [ChIP] after RNAi) or with no transfection (ChIP only). Cells were serum starved overnight, followed by 10 min of serum stimulation or mock treatment. Cells were washed twice with PBS and cross-linked with 1% formaldehyde at room temperature for 10 min. Cells were then rinsed with ice-cold PBS twice, collected into 100 mM Tris-HCl (pH 9.4)–10 mM dithiothreitol, incubated for 15 min at 30°C, and centrifuged for 5 min at 2,000 × *g*. Cells were washed sequentially with 1 ml of ice-cold PBS, buffer I (0.25% Triton X-100, 10 mM EDTA, 0.5 mM EGTA, 10 mM HEPES, pH 6.5), and buffer II (200 mM NaCl, 1 mM EDTA, 0.5 mM EGTA, 10 mM HEPES, pH 6.5). Cells were resuspended in 0.3 ml of lysis buffer (1% SDS, 10 mM EDTA, 50 mM Tris-HCl [pH 8.1], 1× protease inhibitor cocktail [Roche]) and sonicated

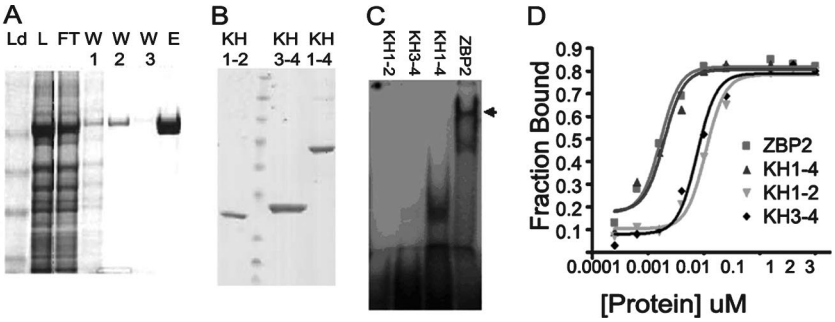

FIG. 1. ZBP2 binds to the chicken β-actin zipcode with all four KH domains. (A) Purification of ZBP2 from SF9 insect cells. His-tagged ZBP2 (lane E) was purified from insect cell lysates (lane L) after three washes (lanes W1 to W3). Ld is benchmark protein ladder (Invitrogen). (B) Three ZBP2 truncations, i.e., the first and second KH domains (KH1-2), the third and fourth KH domains (KH3-4), and all four KH domains (KH1-4), were expressed and purified using the same system as for panel A. Ld indicates a 10-kDa protein ladder (Invitrogen). (C) Gel shift with ^{32}P-labeled chicken β-actin zipcode probe using various truncations of ZBP2 KH domains. The full-length ZBP2-zipcode complex is indicated by an arrow. All four KH domains of ZBP2 were required for efficient binding. (D) Nitrocellulose filter binding assay of the ZBP2 fragments in panel C, showing affinity curves for the β-actin mRNA zipcode. Recombinant full-length ZBP2 and three fragments, i.e., KH1-2, KH3-4, and KH1-4, at various concentrations were incubated with ^{32}P-labeled zipcode RNA probe. Bound probe was detected by Cerenkov counting after binding of the protein-RNA complex to the filter and intensive washing.

three times for 10 s each at the maximum setting, followed by centrifugation for 10 min at 15,000 rpm. Supernatants were collected and diluted in buffer (1% Triton X-100, 2 mM EDTA, 150 mM NaCl, 20 mM Tris-HCl, pH 8.1), followed by immunoclearing with 2 μg sheared salmon sperm DNA, 20 μl preimmune serum, and protein A-Sepharose (45 μl of a 50% slurry in 10 mM Tris-HCl [pH 8.1] and 1 mM EDTA) for 2 h at 4°C. Immunoprecipitation was performed overnight at 4°C with specific antibodies. In some experiments, supernatants were pretreated with RNase A (10 μg/ml) for 1 hour on ice before incubation with antibodies. After immunoprecipitation, 45 μl protein A-Sepharose slurry was added, and the incubation was continued for another 1 h. Precipitates were washed sequentially for 10 min each in TSE I (0.1% SDS, 1% Triton X-100, 2 mM EDTA, 20 mM Tris-HCl [pH 8.1], 150 mM NaCl), TSE II (0.1% SDS, 1% Triton X-100, 2 mM EDTA, 20 mM Tris-HCl [pH 8.1], 500 mM NaCl), and buffer III (0.25 M LiCl, 1% NP-40, 1% deoxycholate, 1 mM EDTA, 10 mM Tris-HCl [pH 8.1]). Precipitates were then washed three times with TE (10 mM Tris [pH 7.4], 1 mM EDTA) buffer and extracted three times with 1% SDS–0.1 M NaHCO3. Eluates were pooled and heated at 65°C for at least 6 h to reverse the formaldehyde cross-linking. DNA fragments were purified with a QIAquick spin kit (QIAGEN). For PCR, 1 μl from a 50-μl DNA extraction and 20 to 25 cycles of amplification were used.

RESULTS

The four KH domains of ZBP2 are required for zipcode binding. We have previously determined ZBP2 protein expression levels in developing chicken brain lysates (23). Examining the expression profile of ZBP2 (KSRP) in a variety of human tissues showed that ZBP2/KSRP mRNA levels were higher in tissues with more β-actin mRNA, suggesting that the expression of KSRP/ZBP2 is correlated with that of β-actin (see Fig. S1 in the supplemental material). ZBP2 and ZBP1 each have four KH domains responsible for RNA binding (8). For ZBP1, KH domains 3 and 4, but not 1 and 2, are essential for zipcode binding in vitro, mRNP particle formation, and cytoskeletal attachment in vivo (18). To test which domains within ZBP2 were responsible for binding to the zipcode, we expressed and purified recombinant ZBP2 and KH domain fragments. Full-length ZBP2 could not be efficiently expressed in *Escherichia coli*, presumably because of its GC-rich regions which encoded proline and arginine (23). Therefore, we chose insect cells to express ZBP2 and obtained full-length protein with a satisfactory yield. A lysate of SF9 cells expressing His-tagged ZBP2 (Fig. 1A, lane L) was incubated with Ni-nitrilotriacetic acid beads, and nonspecific proteins bound to beads were removed by intensive washing (lanes W1 to 3). His-tagged ZBP2 (lane E) was eluted, concentrated, and analyzed by SDS-PAGE to be over 95% pure. We also expressed three ZBP2 truncations, i.e., the first and second KH domains (KH1-2), the third and fourth KH domains (KH3-4), and all of the domains (KH1-4), to test their RNA binding affinity (Fig. 1B). We determined that all four KH domains of ZBP2 were required for efficient binding to chicken β-actin zipcode in gel shift experiments. The first two KH domains (KH1-2) or the third and fourth KH domains (KH3-4) did not have strong binding, while KH1-4 and the full-length protein (ZBP2) bound more efficiently (Fig. 1C). Nitrocellulose filter binding assays were then used to calculate the binding affinities of ZBP2 and its truncations to the zipcode. Recombinant full-length ZBP2, KH1-2, KH3-4, or KH1-4 was incubated with ^{32}P-labeled zipcode RNA probe at various concentrations. Bound probe was detected by Cerenkov counting after binding of the protein-RNA complex to the filters and intensive washing. The dissociation constant (K_d) was then plotted from the association curve. Full-length ZBP2 and KH1-4 have a K_d of around 10 nM, while KH1-2 and KH3-4 have K_ds approximately 10 times higher, indicating that efficient RNA binding of ZBP2 requires all KH domains (Fig. 1D).

ZBP2 binds to pyrimidine rich sequences. ZBP2 bound to the zipcode of β-actin mRNA but did not bind to a mutated zipcode incapable of asymmetrically localizing a reporter (23). The exact sequences that ZBP2 recognized were unknown. Thus, we used SELEX to specifically amplify RNA ligands of ZBP2 (9, 17). RNAs in vitro transcribed from a random 20-mer SELEX pool were incubated with full-length ZBP2. The protein-RNA complexes were collected with a nitrocellulose filter and then amplified by RT-PCR. and in vitro transcribed into RNAs for another round of selection. With this approach, we analyzed 14 PCR products after 10 rounds of amplification. Sequence analysis revealed that 11 of them fell into two groups. One group contained a CCCC motif while the other group contained a GUCC motif (Fig. 2A) near their 3′ ends. Noticeably, we did not find a degenerate ACACC conserved

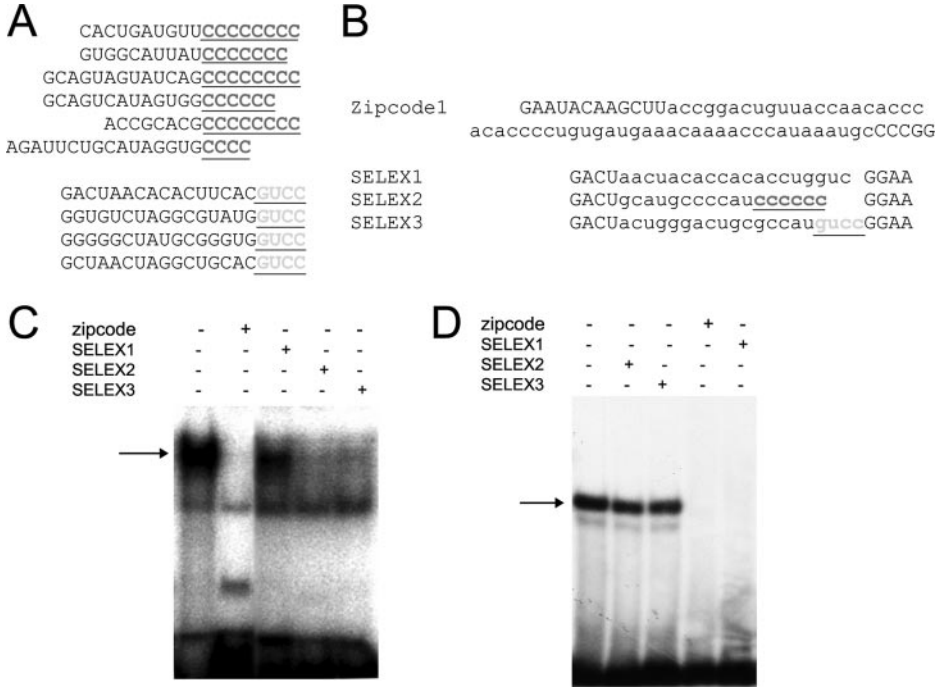

FIG. 2. ZBP2 binds to pyrimidine-rich RNA ligands. (A) SELEX was used to select RNA motifs specifically recognized by ZBP2. After 10 rounds of selection and amplification, 20 clones were sequenced, and two groups with conserved patterns are aligned and underlined: the CCCC motif and the GUCC motif. (B) RNA competitor sequences used for panels C and D. The zipcode was in vitro transcribed as described in Materials and Methods. SELEX competitors were in vitro transcribed from PCR products amplified from SELEX clones S1 (ZBP1 SELEX), S2, and S3 by T7 polymerase. (C) RNA competition shows that the two SELEX oligonucleotides efficiently competed with the zipcode for ZBP2 binding. No competitor or 100× concentrations of different competitors were preincubated with ZBP2 for 15 min. ^{32}P-labeled chicken β-actin zipcode probe was added to the mix and incubated for a further 30 min. The RNA-protein complexes were resolved in a 6% native gel. The arrow indicates the position of the ZBP2-zipcode complexes. (D) Binding of the zipcode to ZBP1 was not competed with the CCCC or GUCC motif. RNA competition assays were performed as for panel C. The position of the ZBP1-zipcode complexes is indicated.

motif in this amplification as was found using the KH3-4 domain of ZBP1 as a bait (18). In order to verify the specificity of binding of ZBP2 to the CCCC- and GUCC-containing SELEX clones, we performed two RNA competition experiments (Fig. 2C and D). RNA competitors used in the experiments were full-length chicken zipcode; a 27-mer RNA fragment with two ACACC repeats but without any of the two conserved ZBP2 binding sequence motifs, which was identified using full-length ZBP1 in a SELEX assay (SELEX1) (S. Hüttelmaier et al., unpublished data); and RNAs transcribed from two SELEX clones containing CCCC and GUCC motifs, respectively (SELEX2 and SELEX3) (Fig. 2B). Different competitors were preincubated with recombinant ZBP2 or ZBP1 for 15 min. A ^{32}P-labeled chicken β-actin zipcode probe was then added to the mix and incubated for a further 30 min. The RNA-protein complexes were resolved in a 6% native gel. Both the CCCC motif and the GUCC motif competed efficiently for zipcode binding of ZBP2 (Fig. 2C). However, these motifs were not able to specifically compete with the zipcode for ZBP1 binding (Fig. 2D). Quantification showed that the efficiency of binding of ZBP1 to the zipcode was decreased only modestly (15% and 16%, respectively) when a 100× excess of the CCCC or GUCC motif was used (Fig. 2D, compare lane 1 with lanes 2 and 3, respectively), suggesting that the motifs were ZBP2 specific. There is a CCCC motif that extends the second ACACCC on the wild-type chicken zipcode, possibly indicating that it could be a ZBP2 binding site. To identify whether this CCCC-containing region was responsible for ZBP2 binding, we generated a mutant zipcode in which the CCCC motif was mutated to GGGG. We found that the mutation affected zipcode binding of both ZBP2 and ZBP1 (data not shown). We reasoned that this effect resulted from the disruption of the secondary structure of the zipcode, which was also important for ZBP1 binding. In addition, structural prediction (RNAfold) suggested that the ZBP1-specific SELEX1 clone forms a stable stem-loop structure, with the first copy of ACACC on the double-stranded stem and the second copy of ACACC on a small loop (data not shown). In contrast, neither SELEX2 nor SELEX 3 could form stable stem-loop structures (data not shown). Together, these findings suggested that ZBP2 most likely bound to a CCCC motif in single-stranded RNAs.

ZBP2 stabilizes a double-stranded RNA stem-loop structure. The different consensus sequences for ZBP1 and ZBP2 binding suggested that they could bind to different sites on the zipcode. In order to determine the precise binding sites of ZBP1 and ZBP2 on the chicken β-actin zipcode, an RNase footprinting assay was performed. The 5′-labeled zipcode probe was incubated with ZBP2 or ZBP1 before digestion by several RNases. A double-stranded-RNA-specific enzyme, RNase V1, showed the best consistency and specificity. After incubation, the reaction products were precipitated, denatured, and resolved on gels. ZBP1 protected a 7-nt region

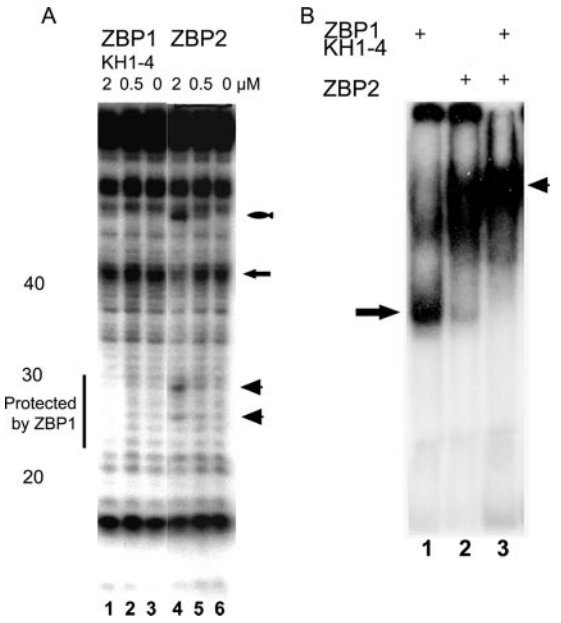

FIG. 3. Recombinant ZBP2 and ZBP1 do not simultaneously bind to the zipcode. (A) RNA footprinting assays using V1 nuclease digestion to determine the binding sites for ZBP1 and ZBP2 on the 54-nt zipcode of chicken β-actin mRNA. ZBP2 increased RNase V1 digestion efficiency in the ZBP1 binding region, resulting in stronger bands (arrowheads and torpedo) as well as a moderate protection of additional bands (arrow). (B) The ^{32}P-labeled chicken 56-nt zipcode was incubated with recombinant ZBP1 KH1-4, ZBP2, or both proteins and then resolved on a 6% native gel. ZBP1 KH1-4 bound to the probe most likely as a monomer (arrow), with minor signal above, presumably ZBP1 dimers. The results indicated that in solution, when both ZBP1 and ZBP2 were present, the zipcode preferentially bound to recombinant ZBP2 (arrowhead).

including the first conserved motif of ACACCC of the chicken zipcode, which had been shown to be important for its functionality (Fig. 3A, lane 1). Interestingly, ZBP2 increased RNase V1 digestion efficiency in the ZBP1 binding region, resulting in stronger bands as well as a moderate protection of additional bands. When the probe was preincubated with both proteins, a digestion pattern similar to that of ZBP2 alone was obtained (data not shown). A band mobility shift experiment was also performed in which ZBP2, ZBP1 KH1-4, or both proteins were incubated with the chicken zipcode probe and then resolved on a native gel. One band was detected for ZBP2 binding (Fig. 3B), as seen in Fig. 2. ZBP1 KH1-4 bound to the probe most likely as a monomer (Fig. 3B, lane 1), with a minor signal above, presumably ZBP1 dimers. When both ZBP2 and ZBP1 were available, only ZBP2 bound to and shifted the zipcode probe (Fig. 3B, lane 3). These data suggested a few in vitro characteristics of ZBP binding to the zipcode. First, recombinant ZBP2 and ZBP1 did not bind simultaneously to the zipcode or bind to the same sequence motif on the zipcode because they did not recognize the same region. Second, ZBP2 bound the zipcode and stabilized nearby double-stranded structures, thus making the zipcode a better substrate for RNaseV1. Third, when both recombinant ZBP2 and ZBP1 were present, ZBP2 preferentially bound the zipcode and was retained on it. This retention could prevent the subsequent association of recombinant ZBP1 to the zipcode, and thus the ZBP1 protection was not observed for the first ACACC motif.

Cloning of mKSRP. Although CEFs are a model system preferably used to study mRNA localization in nonneuronal cells, they have some limitations. Few chicken gene expression profiles are available for analysis. NG108-15 can differentiate to a neuron-like phenotype in vitro (26). Recent studies revealed that similar to the case for primary neurons, β-actin mRNA was localized to the cell periphery and neurites upon inducing differentiation (28). To study the role of ZBP2 in these cells, the mZBP2 orthologue was cloned. mZBP2 has a domain structure similar to that of human KSRP and chicken ZBP2 (see Fig. S3A in the supplemental material). It shares 97% sequence identity with human KSRP on the amino acid level. The homology is 60% with FBP1 and 49% with FBP3, respectively. mZBP2 was expressed in all mouse cell lines we tested, including 3T3, C2C12, NG108-15, and N1E-115 cells (46), with the highest expression in NG108-15 cells (see Fig. S3B in the supplemental material). Analysis of the subcellular distribution of endogenous ZBP2 by indirect immunofluorescence revealed colocalization with a transiently expressed green fluorescent protein (GFP)-tagged mZBP2 fusion protein. Endogenous mZBP2, as the GFP-fused mZBP2 protein, formed nuclear foci that localized around nucleoli (see Fig. S3C and D in the supplemental material). These findings were in agreement with previous reports demonstrating the localization of KSRP to perinucleolar centers and other nuclear foci (25, 27).

ZBP2 binds to nascent β-actin mRNA cotranscriptionally. To test whether ZBP2 is recruited to β-actin mRNAs cotranscriptionally before the nascent transcripts are released from the sites of transcription, we performed ChIP experiments. We used mouse cells in ChIP experiments based on the ease of obtaining large amounts of material, the fact that localization of β-actin mRNA in the cells was also ZBP1 and ZBP2 dependent, and the fact that expression of the β-actin gene could be serum induced. MTC cells were serum starved overnight, followed by either mock treatment or serum stimulation to activate β-mRNA transcription for 15 min before formaldehyde cross-linking. Equal amounts of anti-mZBP2 antibody, normal rabbit immunoglobulin G (IgG) or antihistone antibody were used for immunoprecipitation. Two primer pairs were designed to amplify the 5′ or 3′ region of the β-actin-coding sequence, with expected sizes of 170 bp and 130 bp, respectively. ZBP2 antibody was able to precipitate only the chromatin region comprising the 3′-end of the β actin gene, including the stop codon as well as the adjacent zipcode (Fig. 4A, upper panel). In contrast, the 5′ region of the β-actin-coding sequence was not isolated in the control of ZBP2 pulldowns (Fig. 4A, lower panel). Notably, the association of ZBP2 with the chromatin region comprising the β-actin 3′ end was observed only upon serum stimulation.

ZBP2 and ZBP1 colocalize in nuclear foci with nascent β-actin mRNA. Recent studies revealed that ZBP1 is a nuclear-cytoplasmic shuttling protein and is recruited to β-actin transcription sites upon serum stimulation (42). ZBP1–β-actin particles are then probably coexported into the cytoplasm and localized to the cell periphery by a motor-driven process (37). To determine if ZBP2 was targeted to β-actin transcription sites as well, yellow fluorescent protein-ZBP1 and cyan fluo-

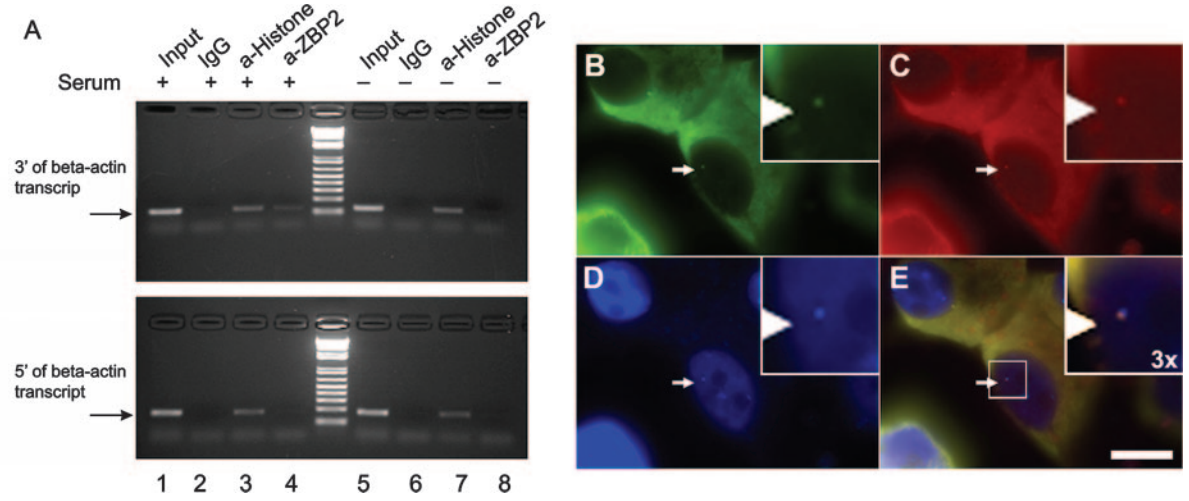

FIG. 4. ZBP2 binds to and colocalizes with nascent β-actin mRNA. (A) MTC cells, which were serum responsive, were either serum starved overnight or stimulated with serum for 15 min. The cells were subjected to ChIP using anti-acetylated histone antibody, normal rat IgG, or polyclonal antibodies against the C terminus of mZBP2 (a generous gift from Doug Black). Two primer pairs, one amplifying the 3′ end of the β-actin-coding region and the other amplifying the 5′ end, which was approximately 3 kb upstream of stop codon, were used in PCR experiments after ChIP. mZBP2 was associated only with the 3′ end of the β-actin-coding region after serum stimulation (A, upper panel, arrow) and not with the 5′ end (A, lower panel, arrow). (B to E) ZBP2 and ZBP1 colocalize at the β-actin mRNA transcription site. Yellow fluorescent protein-ZBP1 (green) (B) and cyan fluorescent protein-mZBP2 (blue) (D) were cotransfected overnight into NG108 cells. Cells were plated on Cell-Tek (BD Bioscience)-coated coverslips and then serum starved for 12 h for differentiation. Nuclear foci were observed with colocalization (arrow) of ZBP1 (B), ZBP2 (D), and β-actin mRNA (red) (C). The merged image is shown in panel E. Bar, 10 μm.

rescent protein-mZBP2 were cotransfected into NG108-15 cells. Both ZBP1 and ZBP2 were localized to active β-actin transcription sites identified by in situ hybridization with the β-actin probe (Fig. 4B to E; additional representative images are shown in Fig. S4 in the supplemental material). Nuclear β-actin mRNA loci representing transcription sites were detected in only 3 to 5% of differentiating NG108-15 cells cultured in low-serum medium. These data suggest that ZBP2 and ZBP1 can transiently coassociate with β-actin mRNA in a transcription-dependent manner.

Loss of ZBP2 function reduces efficiency of binding of ZBP1 to β-actin transcription sites. RNAi is a convenient and powerful way to study loss of protein function in cultured cells (15, 16). To knockdown the endogenous ZBP2, siRNAs were applied to induce mRNA degradation in cell lines from different species. The N-terminal siRNA was directed against the mouse and rat ZBP2, while another siRNA was directed against a region comprising the KH domains of the mouse, rat, and human ZBP2. Western blotting revealed that upon transfection in human 293 cells, only the KH-siRNA induced knockdown of ZBP2 (Fig. 5A). Normalization of vinculin protein levels identified a knockdown of ZBP2 protein levels of approximately 70%, while the control protein remained unaffected. Likewise, the siRNA-transfected 293 cells were subjected to real-time quantitative RT-PCR, which identified a specific degradation of the ZBP2 mRNA, while the ZBP1 mRNA remained unaffected (Fig. 5B). Several other mRNAs were monitored in these experiments, including GAPDH (glyceraldehyde-3-phosphate dehydrogenase) mRNA, and none was significantly affected in its ratios. In NG108-15 cells, the KH-siRNA also efficiently reduced ZBP2 protein levels, as demonstrated by Western blotting (not shown). We then performed in situ hybridization with a β-actin probe on differentiated NG108-15 cells transfected with GFP-ZBP1 and siRNA directed against ZBP2. In scramble, siRNA-untreated cells, 4% showed colocalization of ZBP1 at the β-actin transcription sites. (Representative images are shown in Fig. S5 in the supplemental material.) The lower percentage of cells with β-actin transcription sites was due to the fact that cells were not serum synchronized and β-actin genes were turned on only in a small percentage of individual cells when they were fixed. However, colocalization of ZBP1 and nascent β-actin mRNA was significantly reduced to 0.3% in cells when ZBP2 was knocked down (Fig. 5C) ($P < 0.001$). This result indicated that the reduced recruitment of ZBP1 to β-actin transcription sites may have resulted from the loss of ZBP2 function.

ZBP2 facilitates the recruitment of ZBP1 to nascent β-actin mRNA. We employed the following approaches to further determine whether ZBP2 played a role in facilitating ZBP1 binding to newly transcribed β-actin mRNA. First, we detected dynamic recruitment of ZBP1 and ZBP2 to β-actin transcription sites using serum stimulation after synchronization by serum starvation. If ZBP2 was necessary for ZBP1 to bind to nascent mRNA, it would be expected that ZBP2 would precede ZBP1 binding at the transcription sites. CEFs were serum stimulated and fixed at 5-min intervals and subjected to in situ hybridization with the β-actin RNA probe and immunofluorescence with ZBP1 and ZBP2 antibodies. Analyses of cells with a nuclear ZBP1 signal showed a peak of ZBP2 and β-actin RNA colocalization after 10 min of serum stimulation. In contrast, ZBP1 appeared at transcription sites about 6 min later, indicating that ZBP1 was probably associated with β-actin mRNPs thereafter (Fig. 6A). These results suggested that association of ZBP2 with the nascent β-actin transcripts preceded ZBP1. Second, we performed combined assays with ChIP and PCR analysis in ZBP2 knockdown MTC cells (Fig.

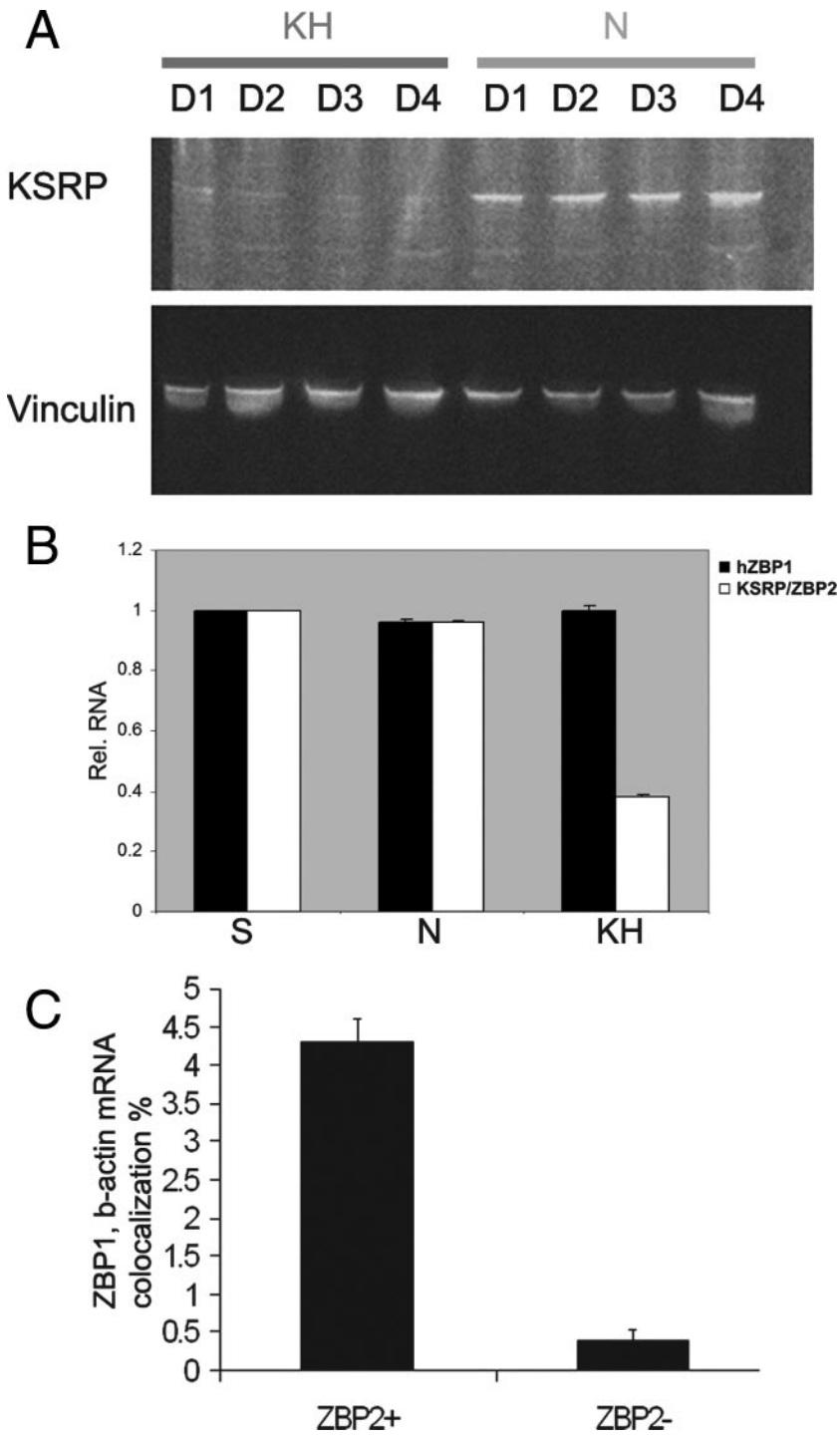

FIG. 5. Efficient knockdown of ZBP2 by RNAi. (A) RNAi effect caused by ZBP2 siRNAs in 293 cells. siRNA oligonucleotides against the KH domain or the N terminus of ZBP2/KSRP were transfected overnight into HEK293 cells with Lipofectamine 2000. Cells were aliquoted to six-well plates, and samples were collected for whole-cell lysates and total RNA preparation at 24, 48, 72, and 96 h after plating (D1 to -4). A monoclonal antibody was used in the Western blot to detect KSRP/ZBP2 expression, whereas vinculin was used as loading control. (B) ZBP2 mRNA was degraded by siRNA against the KH domain of KSRP/ZBP2. A scrambled siRNA (S) N-terminal ZBP2 siRNA (N), or KH domain ZBP2 siRNA (KH) was transfected into 293 cells as described above, and total RNA was isolated, reverse transcribed, and subjected to real-time PCR. ZBP1 (black) and ZBP2 (white) relative mRNA levels were normalized and averaged from the values from three independent experiments. Error bars indicate standard deviations. (C) Colocalization of ZBP1 and β-actin mRNA at the transcription sites requires ZBP2. NG108-15 cells were transfected with ZBP2 KH domain siRNA and differentiated as described in Materials and Methods. After in situ hybridization against β-actin mRNA, the percentage of cells with ZBP1 colocalized with transcription sites was counted in cells with ZBP2 (ZBP2+) or without ZBP2 (ZBP2−) after RNAi ($P < 0.001$).

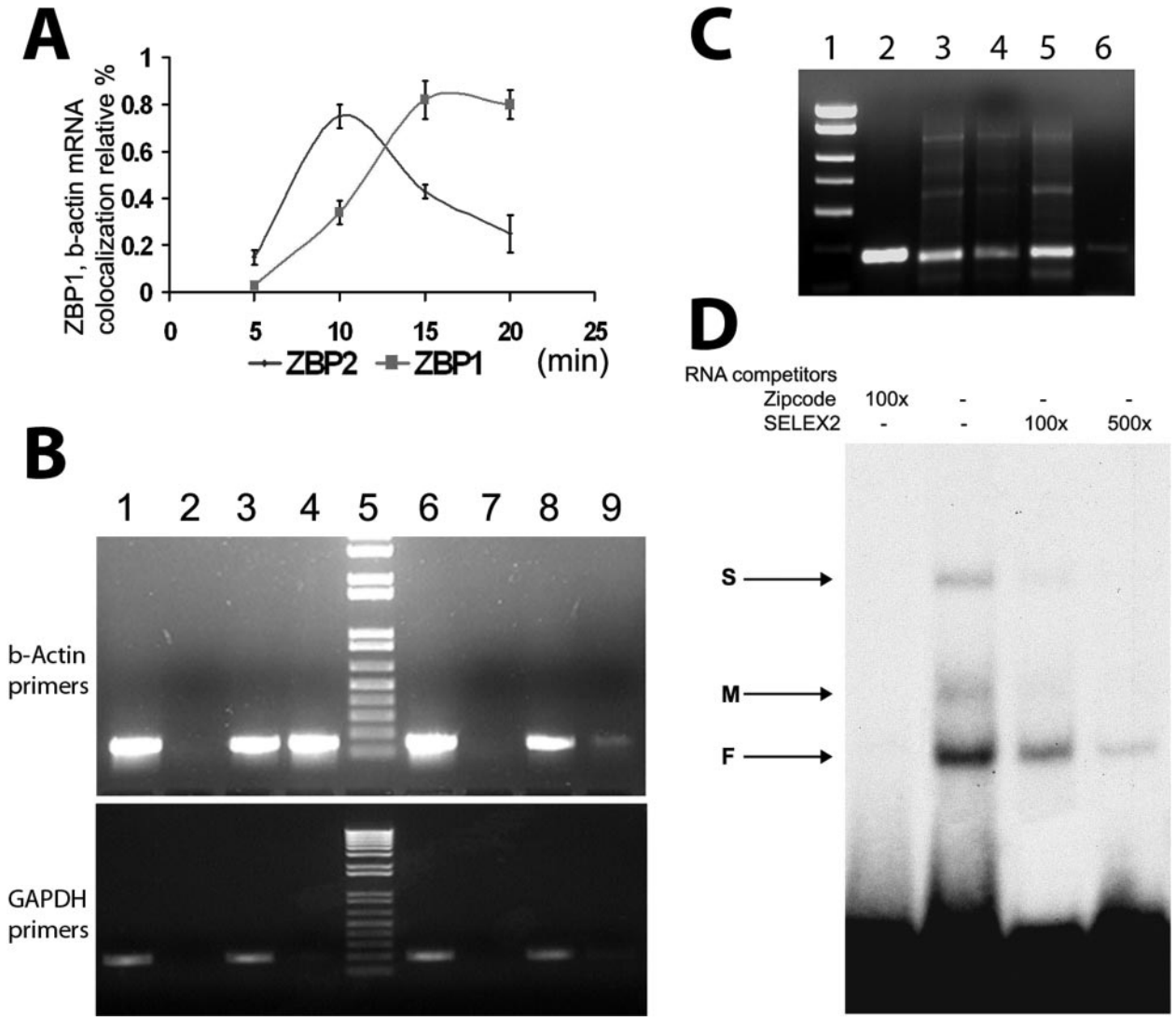

FIG. 6. ZBP1 recruitment to β-actin transcription sites is ZBP2 dependent. (A) Time course of ZBP1 and ZBP2 recruitment. CEFs synchronized by serum starvation were serum stimulated and then fixed at 5-min intervals. At least 200 cells with ZBP1 and ZBP2 signals were counted at each time point. The diagram shows the average percentage of cells with ZBP1 or ZBP2 colocalized with β-actin nascent transcripts from two independent experiments. Error bars indicate standard deviations. (B) ZBP2 is required for efficient binding of ZBP1 to nascent β-actin mRNA. MTC cells were transfected with either scrambled RNAi oligonucleotide (lanes 1 to 4) or ZBP2 RNAi oligonucleotide (lanes 6 to 9) for 2 days and subjected to ChIP. Two primer pairs were used to amplify the 3′ coding regions of the β-actin (top) and GAPDH (bottom) genes from the precipitates. Lanes 1 and 6, inputs of total nuclear lysates; lanes 3 and 8, anti-acetylated histone antibody was used as positive control; lanes 2 and 7, normal rat IgG was used as negative control. Lanes 4 and 9 used polyclonal antibodies against chicken ZBP1. Binding of the β-actin gene with acetylated histone was unaffected in the ZBP2 knockdown cells (compare lane 3 to lane 8). However, knockdown of ZBP2 expression reduced the binding of ZBP1 to nascent β-actin mRNA by 65% (compare lane 4 to lane 9). (C) Chromatin lysates from cultured MTC cells were treated with RNase A and subjected to precipitation with antibodies against histone (lanes 3 and 4) and ZBP1 (lanes 5 and 6). The precipitation efficiency of ZBP1 with the β-actin gene was drastically affected in the RNase A-treated cell lysates, indicating that their association is transcription dependent. Lane 2 indicates the lysate input. (D) Effective binding of ZBP1 to the zipcode requires ZBP2. CEF extracts were preincubated with 100× unlabeled zipcode and different amounts of CCCC' containing SELEX2 oligonucleotides for 15 min. ^{32}P-labeled chicken β-actin zipcode probe was added to the mixes and incubated for additional 30 min. The RNA-protein complexes were separated in a 6% native gel. The arrows point the positions of the three zipcode complexes (S and M, ZBP2 complexes; F, ZBP1 complex).

6B). We used these mouse cells for the assays because large amounts of material could be obtained and they were more efficient for siRNA transfection. MTC cells, which were transfected with either scrambled siRNAs (lanes 1 to 4) or ZBP2-directed siRNAs (lanes 6 to 9) for 2 days, were subjected to ChIP. Anti-acetylated histone antibody (lanes 3 and 8) or normal rat IgG (lanes 2 and 7) was utilized as a positive or negative control, respectively. A β-actin primer pair was employed to amplify the 3′ end of the gene (Fig. 6B, top), and another primer pair was synthesized to amplify a 3′ end of the GAPDH gene, with an estimated size of 220 bp (Fig. 6B, bottom), using the precipitates as templates. The results demonstrated that anti-acetylated histone antibody precipitated both the β-actin and GAPDH genes (lane 3), while the anti-

ZBP1 antibody was able to pull down the 3′ end of the β-actin gene only when ZBP2 was present (lane 4). Knockdown of ZBP2 noticeably reduced the binding of ZBP1 to nascent β-actin mRNA, by 65% (compare lane 4 to lane 9). However, association of the gene with acetylated histone was unaffected in the ZBP2 knockdown cells (compare lane 3 to lane 8). Precipitation of β-actin transcripts by ZBP1 antibody apparently was RNA dependent, since pretreatment of cell lysates with RNase A decreased the precipitation efficiency by over 70% (Fig. 6C, compare lane 5 to lane 6), These results indicated that ZBP1 and β-actin mRNA were physically associated at transcription sites and moreover strongly suggested that ZBP2 was essential for regulating this association. Third, we carried out RNA gel shift assays in the presence of RNAs specifically competing the binding of ZBP2 to the zipcode to test whether ZBP2 was required to facilitate ZBP1 binding to the zipcode. We previously identified three bands of RNA-zipcode complexes when incubating CEF extracts with radiolabeled zipcode probe (23). The F complex corresponded to an interaction between ZBP1 and the zipcode. The M and S complexes were ZBP2 specific. We reasoned that if the binding of ZBP1 to the zipcode was ZBP2 dependent, competing with ZBP2-zipcode RNA binding would affect the formation of the ZBP1-zipcode complex in CEF extracts. To address this, CEF extracts were preincubated with different amounts of ZBP2-specific CCCC motif containing SELEX2 RNAs or with a 100× molar excess of wild-type β-actin zipcode for 15 min. ^{32}P-labeled zipcode probe was then added to the mix and incubated for additional 30 min. As expected, competition for ZBP2 to the zipcode not only abolished the formation of the ZBP2-zipcode complex (Fig. 6D, complexes M and S) but also significantly affected the binding of ZBP1 to the zipcode (complex F). A quantification revealed that the binding of ZBP1 to the zipcode was reduced by 48% and 79% in the presence of 100× and 500× excesses of CCCC-containing SELEX2 sequence, respectively (Fig. 6D). In comparison, competition with unlabeled zipcode completely abolished the formation of both ZBP2-zipcode and ZBP1-zipcode complexes. Hence, the reduced association of ZBP1 with the zipcode in the presence of RNAs specifically competing with the ZBP2-zipcode interaction (Fig. 2C) further supports the hypothesis that ZBP2 is required to facilitate binding of ZBP1 to the zipcode.

Knockdown of ZBP2 affects neurite outgrowth. We expected that ZBP2 knockdown would have physiological consequences in vivo by interfering with the spatio-temporal control of β-actin mRNA expression. NG108-15 cells were transfected with either scrambled siRNA or effective ZBP2 oligonucleotide for 48 h and then differentiated for 12 h. Immunofluorescence was then performed with a monoclonal antibody against KSRP/ZBP2. GFP signal provided a transfection marker (Fig. 7A). Far fewer ZBP2-negative cells than ZBP2-positive cells had elongated neurites (Fig. 7B to D). The analysis of more than 200 cells from two independent experiments showed that 82% of ZBP2-positive cells had neurites longer than 1.5 times the cell diameter of the cell body, while only 33% of ZBP2-negative cells had elongated neurites (Fig. 7E). Similar results were obtained when ZBP1 was knocked down by RNAi (28), suggesting that ZBP1 and ZBP2 were involved in a common pathway affecting neurite outgrowth.

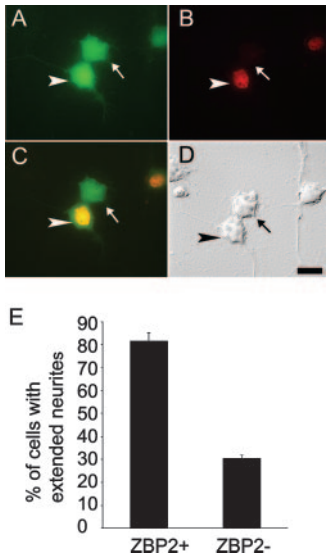

FIG. 7. ZBP2 is required for neurite outgrowth. (A to D) Knockdown of ZBP2 inhibits neurite outgrowth. Differentiating NG108-15 cells were cotransfected with a GFP-expressing plasmid and with either scrambled siRNA or ZBP2 KH domain siRNA for 48 h. The two populations were mixed and plated on Cell-Tek-coated coverslips. Cells were seeded overnight and then subjected to 12 h of differentiation and immunofluorescence detection against ZBP2. GFP (A) (green), ZBP2 (B) (red), merged (C), and differential interference contrast (D) images are shown. ZBP2 knockdown cells (arrows) did not form elongated neurites, in contrast to ZBP2-positive cells (arrowheads). Bar, 10 μm. (E) Statistical analysis of effects of ZBP2 knockdown on neurite growth. More than 80% of the ZBP2-positive (ZBP+) cells have neurites longer than 1.5 times the cell diameter, while only 33% of ZBP2 knockdown (ZBP−) cells have elongated neurites. At least 200 cells were counted in each of three independent experiments. Error bars indicate standard deviations.

DISCUSSION

ZBP2 and ZBP1 are two zipcode binding proteins that have been shown to be essential for the efficient asymmetric localization of β-actin mRNAs (23, 47). ZBP2 is a predominantly nuclear protein, and ZBP1, although detected at β-actin transcription sites (42), is mostly cytoplasmic. In this study, we analyzed the dynamic association of the two proteins with nascent β-actin mRNA. We show that in the nucleus, binding of ZBP2 to the zipcode proceeds ZBP1. Loss of ZBP2 function significantly reduced the efficiency of binding of ZBP1 to the zipcode. We propose that ZBP2 binds initially to the zipcode of a nascent β-actin mRNA, and this process facilitates the subsequent recruitment of ZBP1 to the transcription sites where ZBP1 associates with the RNA and assembles an mRNP complex necessary for the cytoplasmic localization.

Requirement of KH domains of ZBP2 for RNA binding. We have characterized the functional domains of ZBP2 responsible for RNA binding. Unlike KSRP, which requires only KH3-4 for CU-rich element binding (18), ZBP2 binding to the zipcode requires all four KH domains. The requirement of

KH1-2 perhaps allows ZBP2 to maintain the overall structure for binding to specific RNA ligands. This suggests that ZBP2/KSRP from different species recognizes RNA sequences that vary dramatically in primary sequence and secondary structure (20, 23, 35, 45). In addition to the KH domains, a C-terminal glycine- and glutamine-rich domain with four copies of degenerate AWEEYYK motifs could also regulate the sequential binding of ZBP2 and ZBP1 to β-actin mRNA. Overexpression of KH1-4 domains of ZBP2 partially disrupted the cytoplasmic localization of β-actin mRNA (23). The C-terminal sequence is also important for the association of *Drosophila* PSI (ZBP2 homologue) with U1 snRNP, but it is not essential since constructs lacking this sequence are capable of rescuing the lethal phenotype of a PSI null mutation in *Drosophila* (36).

Phenotypes of ZBP2 knockdown by RNAi. A spatial regulation of β-actin protein levels appears to be essential for the regulation of neurite outgrowth and growth cone guidance (28, 52). Neurite outgrowth is disrupted in NG108-15 cells after ZBP2 knockdown. It is difficult to quantify RNA localization in these cells due to heterogeneity of cell morphology, but it was demonstrated in spreading NG108-15 cells that interfering with the regulation of ZBP1 function affects the spatial control of β-actin protein levels (28). Hence, interfering with the loading of ZBP1 on the zipcode-containing RNAs in the nucleus, for instance via ZBP2 knockdown, would perturb spatially restricted translation of the β-actin mRNA (28, 52).

Sequential binding of ZBP2 and ZBP1 to the zipcode of nascent β-actin mRNA. Using SELEX and RNA affinity chromatography assays, KSRP and *Drosophila* ZBP2 have been identified to bind to CU-rich sequences (2, 41). Our work indicates that ZBP2 specifically binds to pyrimidine-rich sequences and ZBP1 preferentially binds to an ACACC motif in the zipcode (18). We propose that ZBP2 and ZBP1 bind sequentially to adjacent but distinct sequence motifs on the zipcode. The chicken zipcode has two adjacent copies of ACACCC motifs, the second of which appears to bind ZBP2. Mammalian zipcodes contain only one copy of ACACCC, but a pyrimidine-rich sequence following the zipcode core motif presumably serves as a putative ZBP2 recognition site. RNase protection supported this hypothesis that ZBP1 and ZBP2 bound to adjacent sequences of the zipcode. The closely apposed binding sites for ZBP1 and ZBP2 presumably make a stable tertiary complex unlikely, containing both proteins with the zipcode RNA. Supportive data for this hypothesis are as follows. First, although ZBP1 or ZBP2 was capable of forming a complex with the zipcode, a ZBP1/ZBP2/zipcode supershift complex was not detected in gel mobility assays using cell extracts. Second, UV cross-linking experiments did not detect ZBP1 and ZBP2 simultaneously associated with the RNA (23). Third, a ZBP1/ZBP2/zipcode supershift complex was also not detected when both recombinant proteins were present with the zipcode in vitro, eliminating the possibility that there might be inhibitors in total cell lysate to prevent tertiary complex formation. Fourth, coimmunoprecipitation or fluorescent resonance energy transfer between ZBP1 and ZBP2 under various conditions was unsuccessful (data not shown). Therefore, we favor a "handover" model in which ZBP1 replaces ZBP2 cotranscriptionally and associates with β-actin mRNA thereafter.

Role of nuclear proteins in cytoplasmic mRNA localization. Colocalization of ZBP2 and cytoplasmic β-actin mRNA is observed in only a small fraction of cells, consistent with a transient interaction (23). We cannot rule out the possibility that improved detection methods may reveal more cells with cytoplasmic ZBP2 that colocalizes with β-actin mRNA, but it is more likely that the protein serves mainly a nuclear role. We suggest that the formation of a prelocasome for β-actin mRNA begins in the nucleus, where the components dynamically change throughout the processing and export of the mRNA. Our data support this argument by showing the sequential association of ZBP2 and ZBP1 with newly transcribed β-actin mRNAs to form a functional mRNP complex.

Other nuclear proteins have been shown to affect cytoplasmic RNA localization. In *Xenopus* oocytes, formation of a core RNP localization complex of PTB/hnRNP I and Vg1RBP/vera with Vg1 RNA initiates in the nucleus (10, 34, 54). The RNP complex, after transport into the cytoplasm, is remodeled, and additional transport factors are recruited (34). In NIH 3T3 cells, nuclear import of AUF1/hnRNP D is a prerequisite for exerting its cytoplasmic function as an mRNA stabilization factor or in participating in mRNA turnover (7). Exon junction proteins are targeted to active transcription sites and may affect the localization potential of a number of mRNAs (11). For example, Y14/magonashi have been shown to be critical for *oskar* mRNA localization in *Drosophila* oocytes (24). Those proteins are generally cotransported with their RNA ligands to specific subcellular regions. In specific cell types, KSRP/ZBP2 is also located in perinucleolar compartments, where it associates with its RNA targets (25).

The nuclear "handover" mechanism of β-actin mRNA from ZBP2 to ZBP1 may require additional factors. However, in our previous experiments, we were able to detect individual ZBP2-zipcode and ZBP1-zipcode shifted bands when CEF extracts were used (23). In solution when only two recombinant ZBP proteins were present, ZBP2 preferentially associated with the zipcode and was retained on it. Therefore, extracts may contain modifying enzymes such as kinases or phosphatases that allow removal of ZBP2 from the zipcode. Supportive evidence for this hypothesis was the association of the zipcode with a large complex of proteins (23) (for instance, the members of the hnRNP D family whose homologues are known to play a role in *Xenopus* Vg1 localization [12], as well as members of the hnRNP A/B family, such as Hrp48, which is important for repressing *oskar* mRNA translation during transport [51]). Although it is not clear how these factors are involved in the "handover" process, their roles in making up β-actin–mRNP complexes in the nucleus may be transient. We speculate that the nuclear "handover" of β-actin mRNA from ZBP2 to ZBP1 is essential to link the formation of an exportable mRNP with the cytoplasmic regulation of the RNA (28). Because ZBP2/KSRP is a splicing factor, it may also function in mRNA splicing. In fact, the various steps and factors involved in the splicing reaction serve as a model for how a succession of proteins bind an RNA. Several hnRNP proteins, such as Squid and hnRNPI/PTB, have been shown to regulate both RNA splicing and localization (22). Interestingly, PTB and ZBP2/KSRP colocalize in nuclei of various cell lines (25). They may label these RNP complexes for subsequent targeting into distinct subcellular regions. ZBP2 is also a member of the FBP

family of proteins. FBP1 and/or FBP3 was copurified in experiments that identified ZBP2/KSRP/FBP2/MARTA as a prominent zipcode binding protein, suggesting that FBPs were involved in mRNA localization with specificity for different mRNAs (35, 45) (see Fig. S1 in the supplemental material). This demonstration of a sequential binding of two proteins to an mRNA to form a localizable RNP visualized in real time suggests that a hierarchy of binding with increasing specificities exists. Further work will be necessary to identify the physiological relevance of this hierarchy.

ACKNOWLEDGMENTS

This work was supported by NIH grant AR41480 to R.H.S.

We thank Doug Black for kindly providing antibodies against KSRP, Shailesh Shenoy for helping prepare the figures, and other members of the lab for helpful discussions.

REFERENCES

1. **Adams, M. D., R. S. Tarng, and D. C. Rio.** 1997. The alternative splicing factor PSI regulates P-element third intron splicing in vivo. Genes. Dev. **11:**129–138.
2. **Amarasinghe, A. K., R. MacDiarmid, M. D. Adams, and D. C. Rio.** 2001. An in vitro-selected RNA-binding site for the KH domain protein PSI acts as a splicing inhibitor element. RNA **7:**1239–1253.
3. **Bassell, G. J., and R. H. Singer.** 2001. Neuronal RNA localization and the cytoskeleton. Probl. Cell Differ. **34:**41–56.
4. **Bassell, G. J., H. Zhang, A. L. Byrd, A. M. Femino, R. H. Singer, K. L. Taneja, L. M. Lifshitz, I. M. Herman, and K. S. Kosik.** 1998. Sorting of beta-actin mRNA and protein to neurites and growth cones in culture. J. Neurosci. **18:**251–265.
5. **Carey, J., V. Cameron, P. L. de Haseth, and O. C. Uhlenbeck.** 1983. Sequence-specific interaction of R17 coat protein with its ribonucleic acid binding site. Biochemistry **22:**2601–2610.
6. **Chen, C. Y., R. Gherzi, S. E. Ong, E. L. Chan, R. Raijmakers, G. J. Pruijn, G. Stoecklin, C. Moroni, M. Mann, and M. Karin.** 2001. AU binding proteins recruit the exosome to degrade ARE-containing mRNAs. Cell **107:**451–464.
7. **Chen, C. Y., N. Xu, W. Zhu, and A. B. Shyu.** 2004. Functional dissection of hnRNP D suggests that nuclear import is required before hnRNP D can modulate mRNA turnover in the cytoplasm. RNA **10:**669–680.
8. **Chen, T., B. B. Damaj, C. Herrera, P. Lasko, and S. Richard.** 1997. Self-association of the single-KH-domain family members Sam68, GRP33, GLD-1, and Qk1: role of the KH domain. Mol. Cell. Biol. **17:**5707–5718.
9. **Conrad, R. C., S. Baskerville, and A. D. Ellington.** 1995. In vitro selection methodologies to probe RNA function and structure. Mol. Divers. **1:**69–78.
10. **Cote, C. A., D. Gautreau, J. M. Denegre, T. L. Kress, N. A. Terry, and K. L. Mowry.** 1999. A Xenopus protein related to hnRNP I has a role in cytoplasmic RNA localization. Mol. Cell **4:**431–437.
11. **Custodio, N., C. Carvalho, I. Condado, M. Antoniou, B. J. Blencowe, and M. Carmo-Fonseca.** 2004. In vivo recruitment of exon junction complex proteins to transcription sites in mammalian cell nuclei. RNA **10:**622–633.
12. **Czaplinski, K., T. Kocher, M. Schelder, A. Segref, M. Wilm, and I. W. Mattaj.** 2005. Identification of 40LoVe, a Xenopus hnRNP D family protein involved in localizing a TGF-beta-related mRNA during oogenesis. Dev. Cell **8:**505–515.
13. **Davis-Smyth, T., R. C. Duncan, T. Zheng, G. Michelotti, and D. Levens.** 1996. The far upstream element-binding proteins comprise an ancient family of single-strand DNA-binding transactivators. J. Biol. Chem. **271:**31679–31687.
14. **Duncan, R., L. Bazar, G. Michelotti, T. Tomonaga, H. Krutzsch, M. Avigan, and D. Levens.** 1994. A sequence-specific, single-strand binding protein activates the far upstream element of c-myc and defines a new DNA-binding motif. Genes Dev. **8:**465–480.
15. **Elbashir, S. M., J. Harborth, W. Lendeckel, A. Yalcin, K. Weber, and T. Tuschl.** 2001. Duplexes of 21-nucleotide RNAs mediate RNA interference in cultured mammalian cells. Nature **411:**494–498.
16. **Elbashir, S. M., J. Harborth, K. Weber, and T. Tuschl.** 2002. Analysis of gene function in somatic mammalian cells using small interfering RNAs. Methods **26:**199–213.
17. **Ellington, A. D., and J. W. Szostak.** 1990. In vitro selection of RNA molecules that bind specific ligands. Nature **346:**818–822.
18. **Farina, K. L., S. Huttelmaier, K. Musunuru, R. Darnell, and R. H. Singer.** 2003. Two ZBP1 KH domains facilitate beta-actin mRNA localization, granule formation, and cytoskeletal attachment. J. Cell Biol. **160:**77–87.
19. **Farina, K. L., and R. H. Singer.** 2002. The nuclear connection in RNA transport and localization. Trends Cell Biol. **12:**466–472.
20. **Gherzi, R., K. Y. Lee, P. Briata, D. Wegmuller, C. Moroni, M. Karin, and C. Y. Chen.** 2004. A KH domain RNA binding protein, KSRP, promotes ARE-directed mRNA turnover by recruiting the degradation machinery. Mol. Cell **14:**571–583.
21. **Gherzi, R., M. Trabucchi, M. Ponassi, T. Ruggiero, G. Corte, C. Moroni, C. Y. Chen, K. S. Khabar, J. S. Andersen, and P. Briata.** 2006. The RNA-binding protein KSRP promotes decay of beta-catenin mRNA and is inactivated by PI3K-AKT signaling. PLoS Biol. **5:**e5.
22. **Goodrich, J. S., K. N. Clouse, and T. Schupbach.** 2004. Hrb27C, Sqd and Otu cooperatively regulate gurken RNA localization and mediate nurse cell chromosome dispersion in Drosophila oogenesis. Development **131:**1949–1958.
23. **Gu, W., F. Pan, H. Zhang, G. J. Bassell, and R. H. Singer.** 2002. A predominantly nuclear protein affecting cytoplasmic localization of beta-actin mRNA in fibroblasts and neurons. J. Cell Biol. **156:**41–51.
24. **Hachet, O., and A. Ephrussi.** 2004. Splicing of oskar RNA in the nucleus is coupled to its cytoplasmic localization. Nature **428:**959–963.
25. **Hall, M. P., S. Huang, and D. L. Black.** 2004. Differentiation-induced colocalization of the KH-type splicing regulatory protein with polypyrimidine tract binding protein and the c-src pre-mRNA. Mol. Biol. Cell **15:**774–786.
26. **Hamprecht, B., T. Glaser, G. Reiser, E. Bayer, and F. Propst.** 1985. Culture and characteristics of hormone-responsive neuroblastoma X glioma hybrid cells. Methods Enzymol. **109:**316–341.
27. **Huang, S.** 2000. Perinucleolar structures. J. Struct. Biol. **129:**233–240.
28. **Huttelmaier, S., D. Zenklusen, M. Lederer, J. Dictenberg, M. Lorenz, X. Meng, G. J. Bassell, J. Condeelis, and R. H. Singer.** 2005. Spatial regulation of beta-actin translation by Src-dependent phosphorylation of ZBP1. Nature **438:**512–515.
29. **Huynh, J. R., and D. St Johnston.** 2004. The origin of asymmetry: early polarisation of the Drosophila germline cyst and oocyte. Curr. Biol. **14:**R438–R449.
30. **Johnstone, O., and P. Lasko.** 2001. Translational regulation and RNA localization in Drosophila oocytes and embryos. Annu. Rev. Genet. **35:**365–406.
31. **Kindler, S., H. Wang, D. Richter, and H. Tiedge.** 2005. RNA transport and local control of translation. Annu. Rev. Cell Dev. Biol. **21:**223–245.
32. **Kislauskis, E. H., X. Zhu, and R. H. Singer.** 1997. Beta-actin messenger RNA localization and protein synthesis augment cell motility. J. Cell Biol. **136:**1263–1270.
33. **Kislauskis, E. H., X. Zhu, and R. H. Singer.** 1994. Sequences responsible for intracellular localization of beta-actin messenger RNA also affect cell phenotype. J. Cell Biol. **127:**441–451.
34. **Kress, T. L., Y. J. Yoon, and K. L. Mowry.** 2004. Nuclear RNP complex assembly initiates cytoplasmic RNA localization. J. Cell Biol. **165:**203–211.
35. **Kroll, T. T., W. M. Zhao, C. Jiang, and P. W. Huber.** 2002. A homolog of FBP2/KSRP binds to localized mRNAs in Xenopus oocytes. Development **129:**5609–5619.
36. **Labourier, E., M. Blanchette, J. W. Feiger, M. D. Adams, and D. C. Rio.** 2002. The KH-type RNA-binding protein PSI is required for Drosophila viability, male fertility, and cellular mRNA processing. Genes Dev. **16:**72–84.
37. **Latham, V. M., E. H. Yu, A. N. Tullio, R. S. Adelstein, and R. H. Singer.** 2001. A Rho-dependent signaling pathway operating through myosin localizes beta-actin mRNA in fibroblasts. Curr. Biol. **11:**1010–1016.
38. **Lellek, H., R. Kirsten, I. Diehl, F. Apostel, F. Buck, and J. Greeve.** 2000. Purification and molecular cloning of a novel essential component of the apolipoprotein B mRNA editing enzyme-complex. J. Biol. Chem. **275:**19848–19856.
39. **Long, R. M., R. H. Singer, X. Meng, I. Gonzalez, K. Nasmyth, and R. P. Jansen.** 1997. Mating type switching in yeast controlled by asymmetric localization of ASH1 mRNA. Science **277:**383–387.
40. **Lyford, G. L., K. Yamagata, W. E. Kaufmann, C. A. Barnes, L. K. Sanders, N. G. Copeland, D. J. Gilbert, N. A. Jenkins, A. A. Lanahan, and P. F. Worley.** 1995. Arc, a growth factor and activity-regulated gene, encodes a novel cytoskeleton-associated protein that is enriched in neuronal dendrites. Neuron **14:**433–445.
41. **Min, H., C. W. Turck, J. M. Nikolic, and D. L. Black.** 1997. A new regulatory protein, KSRP, mediates exon inclusion through an intronic splicing enhancer. Genes Dev. **11:**1023–1036.
42. **Oleynikov, Y., and R. H. Singer.** 2003. Real-time visualization of ZBP1 association with beta-actin mRNA during transcription and localization. Curr. Biol. **13:**199–207.
43. **Oleynikov, Y., and R. H. Singer.** 1998. RNA localization: different zipcodes, same postman? Trends Cell Biol. **8:**381–383.
44. **Palacios, I. M., and D. St Johnston.** 2001. Getting the message across: the intracellular localization of mRNAs in higher eukaryotes. Annu. Rev. Cell Dev. Biol. **17:**569–614.
45. **Rehbein, M., K. Wege, F. Buck, M. Schweizer, D. Richter, and S. Kindler.** 2002. Molecular characterization of MARTA1, a protein interacting with the dendritic targeting element of MAP2 mRNAs. J. Neurochem. **82:**1039–1046.
46. **Richelson, E.** 1973. Regulation of tyrosine hydroxylase activity in mouse neuroblastoma clone N1E-115. J. Neurochem. **21:**1139–1145.
47. **Ross, A. F., Y. Oleynikov, E. H. Kislauskis, K. L. Taneja, and R. H. Singer.**

1997. Characterization of a beta-actin mRNA zipcode-binding protein. Mol. Cell. Biol. **17:**2158–2165.

48. **Shestakova, E. A., R. H. Singer, and J. Condeelis.** 2001. The physiological significance of beta-actin mRNA localization in determining cell polarity and directional motility. Proc. Natl. Acad. Sci. USA **98:**7045–7050.
49. **Snee, M., G. J. Kidd, T. P. Munro, and R. Smith.** 2002. RNA trafficking and stabilization elements associate with multiple brain proteins. J. Cell Sci. **115:**4661–4669.
50. **Takizawa, P. A., A. Sil, J. R. Swedlow, I. Herskowitz, and R. D. Vale.** 1997. Actin-dependent localization of an RNA encoding a cell-fate determinant in yeast. Nature **389:**90–93.
51. **Yano, T., S. Lopez de Quinto, Y. Matsui, A. Shevchenko, and A. Ephrussi.** 2004. Hrp48, a Drosophila hnRNPA/B homolog, binds and regulates translation of oskar mRNA. Dev. Cell **6:**637–648.
52. **Yao, J., Y. Sasaki, Z. Wen, G. J. Bassell, and J. Q. Zheng.** 2006. An essential role for beta-actin mRNA localization and translation in Ca2+-dependent growth cone guidance. Nat. Neurosci. **9:**1265–1273.
53. **Zhang, H. L., T. Eom, Y. Oleynikov, S. M. Shenoy, D. A. Liebelt, J. B. Dictenberg, R. H. Singer, and G. J. Bassell.** 2001. Neurotrophin-induced transport of a beta-actin mRNP complex increases beta-actin levels and stimulates growth cone motility. Neuron **31:**261–275.
54. **Zhang, H. L., R. H. Singer, and G. J. Bassell.** 1999. Neurotrophin regulation of beta-actin mRNA and protein localization within growth cones. J. Cell Biol. **147:**59–70.